

# Cryospheric Applications of MISR Data

A. W. Nolin, J. C. Stroeve, T. A. Scambos, F. Fetterer  
Cooperative Institute for Research in Environmental Sciences  
National Snow and Ice Data Center, 449 UCB  
University of Colorado  
Boulder, CO 80309-0449

**Abstract-** This work is a demonstration of potential uses of combined multiangle and multispectral remote sensing imagery for mapping and characterizing seasonal snow cover, sea ice, and ice sheet surfaces. We use data from the Multiangle Imaging SpectroRadiometer (MISR) and demonstrate how multiangle data can augment multispectral mapping in unique and valuable ways.

## I. INTRODUCTION

Remote sensing using simultaneously acquired multiangle data is a relatively new concept. Most classification algorithms make use of the spectral contrast of features in different wavelength regions. However, recent research indicates that anisotropic scattering from various Earth surface types (e.g. soil, vegetation, cloud, and snow) creates characteristic angular signatures in addition to the better known spectral signatures [1]. Surface roughness also affects the angular pattern of reflectance. Rougher surfaces tend to be more back scattering, even when the material itself may be predominantly forward scattering. Thus, angular data can be used to separate surface types with different textures, given that the characteristic roughness is detectable at the spatial scale of the remote sensing instrument. The objective of this research is to explore how multiangle imagery can be used for cryospheric applications including mapping snow covered area, snow albedo, and ice sheet surface properties, as well as characterizing sea ice types.

## II. APPROACH

### A. Sensor Description

The Multiangle Imaging SpectroRadiometer (MISR) is a pushbroom sensor, with nine cameras aligned along-track in the forward, nadir and aft directions (see Table 1). Each camera has four spectral bands providing simultaneous spectral and angular information. The spatial resolution of the instrument depends on the camera and the spectral band. All cameras have the red band at 275-m resolution. The nadir camera has all four spectral bands at 275-m resolution. The blue, green and near-infrared channels in the other cameras have a resolution of 1.1 km. With its high radiometric resolution, image saturation is not a problem over bright ice- or snow-covered surfaces.

### B. Case Study Areas

We have chosen several case study regions to examine the synergies between multiangle and multispectral data in cryospheric applications. The case study regions include the

Greenland and Antarctic ice sheets; Davis Strait (off of western Greenland); James Bay, Ontario; and the California Sierra Nevada. Table 2 gives image information for each of these study areas.

TABLE 1  
MISR INSTRUMENT CHARACTERISTICS

Camera angles	70.5°, 60.0°, 45.6°, 26.1° (fore and aft), nadir
Spectral bands	448 nm, 558 nm, 672 nm, 866 nm
Pixel size	275 m at nadir and all red bands 1.1 km all other bands and angles
Swath width	360 km
Quantization	14 bits, square-root encoded to 12 bits

TABLE 2  
IMAGES OF STUDY AREAS

Location	Mapping Purpose	Acquisition Date
West Greenland ice sheet	snow albedo ice sheet characterization	12 August 2000
East Antarctic ice sheet	blue ice snow megadunes	12 December 2000 15 October 2000
Davis Strait	sea ice mapping	4 May 2000
James Bay, Ontario	sea ice mapping ice typing	12 April 2000
Sierra Nevada, California	snow covered area snow - cloud discrimination	15 October 2000

### C. Image Processing Methods

Depending on the particular mapping and characterization purposes, different image processing and classification methods were used. For all case studies, we used data at a spatial resolution of 275 m.

To compute snow albedo from multiangle measurements, we first convert at-sensor radiance values to bidirectional reflectance factor (BRF). We then perform atmospheric correction using the 6S model to get the surface hemispherical-directional reflectance factor (HDRF) values. Lastly, we use conversion factors derived from the DISORT

radiative transfer model to compute surface albedo from HDRF. We used data from the location of the CU/ETH camp in western Greenland (69.6°N, 49.3°W).

For ice sheet surface characterization, we applied a simple forward-backward scattering approach for mapping the differences in angular scattering signatures for different image components. RGB image composites were created from composites of the forward, nadir, and backward viewing cameras. We are particularly interested in mapping bare ice, melting snow and dry snow in the transition region from the accumulation zone to the ablation zone on the Greenland ice sheet. In Antarctica, we seek to map blue ice areas, which are important indicators of climate change and have significant impact on surface energy balance [2, 3].

To identify and characterize these unusual megadune features in East Antarctica, we use radiance data from the nadir camera. We follow the approach of [4] and compute a grain size index using the gradient ratio of the Blue and NIR spectral bands. This grain size information allows us to examine the spatial distribution of fine- and coarse-grained snow on the megadunes.

In our classification of snow cover and sea ice, we use linear unmixing [5]. Here, both the spectral and angular signatures are used to discriminate between image components. First, a principal components (PC) transformation is applied to each multiband image to determine which of the angular and spectral bands contain unique information that would contribute to the classification. Image endmembers are then determined from the data and used in the linear unmixing. The contribution of each image component's multispectral-multiangle spectrum to the pixel spectrum is displayed as a fraction image.

### III. RESULTS

#### A. Albedo

MISR data were converted from TOA radiances to surface HDRFs. Conversion factors were then applied to convert the HDRF values to albedo. Fig. 1 shows HDRF values from 1.14 to 0.78 and the converted albedo values with a far smaller range, between 0.82 and 0.78. Such multiangle snow albedo retrievals provide constraints on the albedo determination thereby improving albedo estimations. Best results have been obtained for solar zenith angles less than 70°.

#### B. Ice Sheet Surface Characterization

Over the Greenland ice sheet, dry snow, melting regions and bare ice are easily distinguished from one another using only the angular data (Fig. 2).

In the Pine Island Glacier image from Antarctica (Fig. 3) blue ice regions closely resemble crevassed areas in the spectral image but are easily distinguished in the multiangle image.

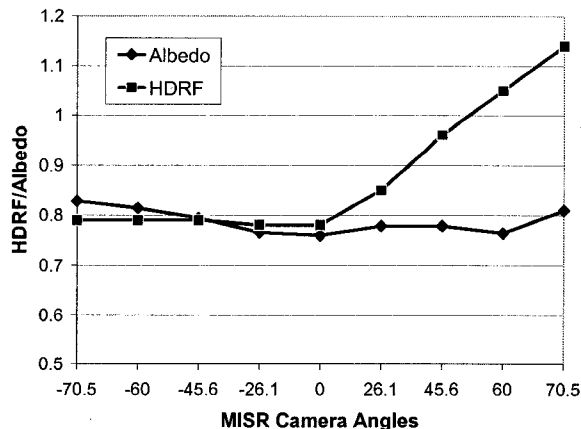


Fig. 1. Surface hemispherical-directional reflectance factor and albedo from the nine MISR cameras (red band only) for the CU/ETH camp in western Greenland (12 August 2000).

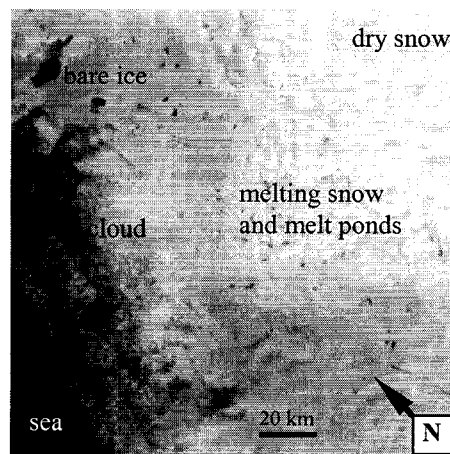


Fig. 2. This multiangle color image acquired over western Greenland shows discrimination between dry snow, melting snow and bare ice based on their angular scattering properties. The 70.5° forward viewing camera is red, the nadir viewing camera is green, and the 70.5° aft viewing camera is blue.

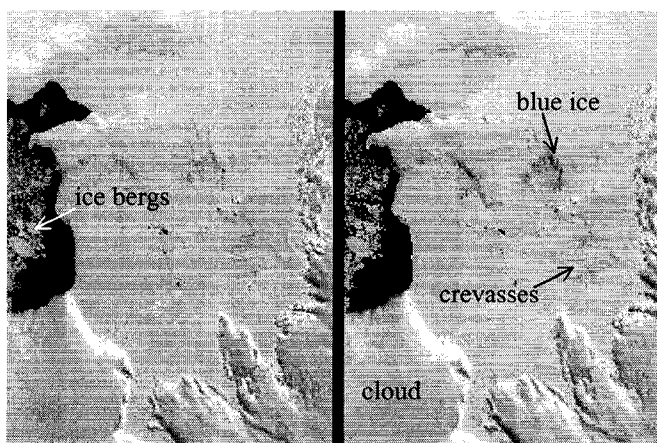


Fig. 3. Pine Island Glacier, Antarctica. The left image is a true color image (RGB). In the right image rough crevassed areas appear orange and are easily distinguished from the smooth blue ice areas shown as dark blue.

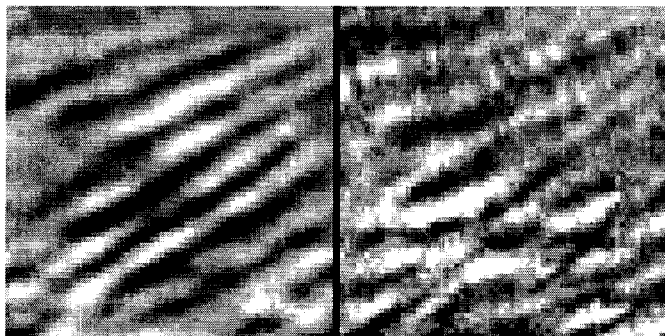


Fig. 4. Blue channel nadir image on left, normalized difference image on right. The image on the right shows relative grain size.

Fig. 4 shows the results of the grain size analysis over the megadunes in East Antarctica. It appears that surface grain size is larger in the troughs than on the dune crests.

### C. Sea Ice Mapping and Ice Typing

Principal components analyses indicate that the angular data contain highly useful information that is different from that of the spectral data. The Davis Strait image (Fig. 5) appears to indicate heterogeneous surface melt on the sea ice. Melting areas show up as dark regions in the near infrared image. The MODIS sea ice temperature product indicates that temperatures were about 272-273 K at the time of image acquisition. The melt signature was strongly evident in the spectral data, confounding the spectral unmixing results. Because the angular signatures were not significantly affected by the melting surface, angular unmixing produced superior discrimination between sea ice, open water, and cloud.

In James Bay (not shown) angular/spectral linear unmixing was able to discriminate not only between ice, cloud and open water, but also between ice types.

### D. Mapping Snow Covered Area

In snow cover mapping over the California Sierra Nevada (not shown), the use of angular data in conjunction with spectral data improved the discrimination between clouds and snow. Linear unmixing results from spectral-only and angular-only unmixing were less accurate than when both spectral and angular information were used. Principal components analysis confirms that angular information is unique from that of the spectral data.

## IV. CONCLUSIONS

This preliminary examination indicates that multiangle data may be used to improve snow albedo retrievals, ice sheet surface characterization, blue ice mapping, sea ice mapping and ice typing. Multiangle data provide additional information that can be valuable for characterizing scenes containing features that exhibit different textural properties that are detectable at the spatial resolution of the sensor.

Future algorithm development for characterization of cryospheric features should include both spectral and angular data.

### ACKNOWLEDGMENT

We thank the Canadian Ice Service for information that aided in interpreting the James Bay image. MISR data were provided through the NASA Langley Distributed Active Archive System. MODIS data were provided by the National Snow and Ice Data Center Distributed Active Archive System (NSIDC-DAAC). Dave Diner provided the Pine Island Glacier image. This work was supported in part by funding from NSIDC-DAAC and NASA grant NAG5-6462.

### REFERENCES

- [1] D. Diner, G. P. Asner, R. Davies, Y. Knyazikhin, J-P. Muller, A. W. Nolin, B. Pinty, C. B. Schaaf, and J. Stroeve, New directions in Earth observing: Scientific applications of multiangle remote sensing, *Bull. Amer. Met. Soc.*, vol. 80, pp. 2209-2228, 1999.
- [2] R. Bintanja, Surface heat budget of Antarctic snow and blue ice: Interpretation of spatial and temporal variability, *J. Geophys. Res.*, vol. 105, pp. 24387-24407, 2000.
- [3] R. Bintanja, S. Jonsson, W. Knap, The annual cycle of the surface energy balance of Antarctic blue ice, *J. Geophys. Res.*, vol. 102, pp. 1867-1881, 1997.
- [4] M. A. Fahnestock, T. A. Scambos, C. A. Shuman, R. J. Arthern, D. P. Winebrenner, and R. Kwok, Snow megadune fields on the East Antarctic Plateau: Extreme atmosphere-ice interaction, *Geophys. Res. Lett.*, vol. 27, pp. 3719-3722, 2000.
- [5] Adams J. B., Smith M. O, and Johnson P. E. (1986) *JGR* 91, 8098-8112.

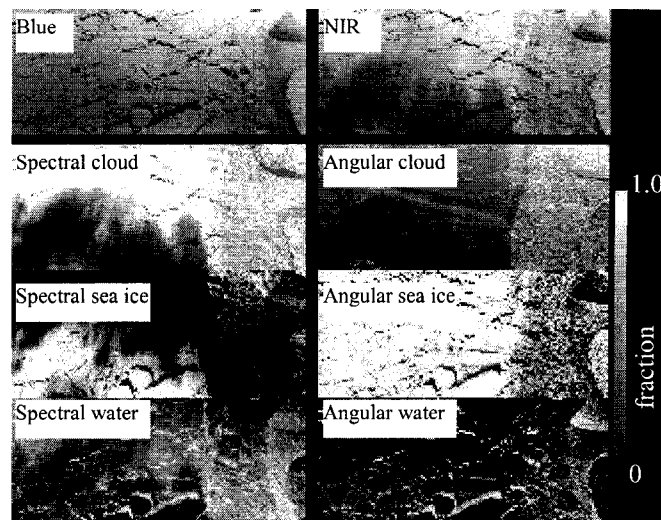


Fig. 5. The top row shows the blue (left) and near-infrared (right) reflectance in the nadir camera. Rows 2-4 show the linear unmixing results for the spectral (left) and angular (right) data. Row 2 is the cloud fraction, row 3 is the sea ice fraction and row 4 is the open water fraction.